AD-A146 621 ESTIMATION OF TARGET POSITIONS USING PLANAR ARRAYS(U) 1/1
ROYAL SIGNALS AND RADAR ESTABLISHMENT MALVERN (ENGLAND)
A R WEBB MAR 84 RSRE-MEMO-3675 DRIC-BR-92463

UNCLASSIFIED F/G 17/9 NL

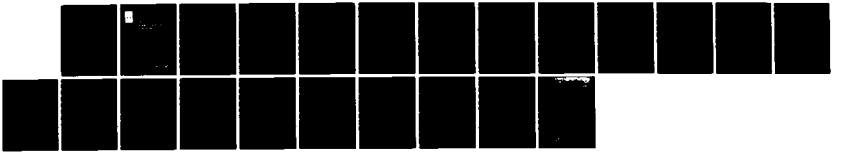

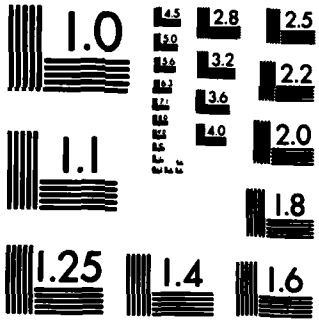

COPY RESOLUTION TEST CHART

RSRE
MEMORANDUM No. 3675

ROYAL SIGNALS & RADAR ESTABLISHMENT

ESTIMATION OF TARGET POSITIONS USING PLANAR ARRAYS

Author: A R Webb

PROCUREMENT EXECUTIVE,
MINISTRY OF DEFENCE,
RSRE MALVERN,
WORCS.

RSRE MEMORANDUM No. 3675

UNLIMITED

UNLIMITED

ROYAL SIGNALS AND RADAR ESTABLISHMENT

Memorandum 3675

Title: ESTIMATION OF TARGET POSITIONS USING PLANAR ARRAYS

Author: A R Webb

Date: March 1984

SUMMARY

Estimation of target position using planar arrays is discussed. For high signal-to-noise ratio, an analytic expression for the rms error in position is derived as a function of the array properties. This is evaluated for various array configurations and it is shown to be approximately constant across the plane of the array. Comparisons are made with arrays in which only pairs of elements are used to estimate position, and it is shown that this may lead to a degradation in performance.

UNLIMITED

RSRE MEMORANDUM 3675

ESTIMATION OF TARGET POSITIONS USING PLANAR ARRAYS

A R Webb

LIST OF CONTENTS

1 Introduction
2 Analysis
3 Signal-to-noise Ratio Definition
4 Analytical Solution
5 Numerical Solution
6 Examples
7 Discussions
8 Conclusions

1 INTRODUCTION

Methods of estimating target position and maintaining a track on a target have been made conventionally using amplitude (or phase) comparison monopulse in which there are two receiver channels for both azimuth and elevation. This method fails when there is more than one target within the scene or when additional signals (multipath, jamming) are present and results in inaccuracies in tracking. It may be possible to overcome these failures by using an array of receivers, which will allow the tracking of many targets simultaneously (Webb, Hearn and Sleigh, 1984). However, it is the purpose of this research note to consider the single target case and to evaluate the tracking error as a function of target position in the scene, array size and signal-to-noise ratio. The reason for the emphasis on the single target situation is that it is likely to occur in many practical radar situations and it is important to understand fully the properties of an array in tracking single targets. The multi-target situation has been considered for a linear array only in RSRE Memorandum 3587 and results for a planar array will be the subject of a separate report. In the following section the equations governing the problem are described and a pair of coupled equations for the azimuth and elevation positions of the target are derived. Section 4 derives an analytic expression for the root mean square tracking errors and this is used in section 6, together with results of a simulation, to illustrate the tracking ability of various array configurations. Finally, we conclude with suggestions for further work and an example of multi-target processing.

The main results of this memorandum show that whilst the rms error in target position is not reduced significantly by employing an array of receivers as opposed to pairs of receivers, the advantages of an array are in allowing accurate target tracking over a wider field of view and in the ability to track many targets simultaneously. Also, arrays based on hexagonal structures offer comparable performance to those based on square lattices but with a reduced density of elements.

2 ANALYSIS

Consider an array of N receivers, each with point-spread function as a function of azimuth and elevation $p_i(\theta,\phi)$ assumed real. Denote the measured output of the array by $\underline{Y} = (y_1 \ldots y_N)$ where y_i is the complex output of receiver i. For a scene consisting of M targets of complex amplitudes A_m ($m = 1, \ldots M$) at positions $\underline{x}_m = (\theta_m,\phi_m)$, the error, $\underline{e}$, between the measured output, $\underline{Y}$, and the outputs for such a scene is given by

$$e_i = \sum_{m=1}^{M} A_m p_i(\underline{x}_m) - y_i \qquad i = 1, \ldots N \qquad (1)$$

For a single target, $M = 1$, of amplitude $A = A_r + iA_i$, we seek a solution which minimises the square error, e^2,

$$e^2 = \underline{e}^T\underline{e}^* = \sum_{i=1}^{N} \{(y_i^r - A_r p_i(\theta,\phi))^2 + (y_i^i - A_i p_i(\theta,\phi))^2\} \qquad (2)$$

where y_i^r, y_i^i are the real and imaginary parts of y_i (in phase and quadrature) and $p_i(\theta,\phi)$ has been assumed real.

Differentiating e^2 with respect to the unknowns A_r, A_i, θ and ϕ, and equating to zero gives a set of four equations in four unknowns. Eliminating A_r and A_i between these, results in a pair of coupled equations for θ and ϕ

$$\sum_{i=1}^{N} \frac{\partial p_i}{\partial \theta}\left[\left(\sum_j p_j^2\right)\left(y_i^r \sum_j p_j y_j^r + y_i^i \sum_j p_j y_j^i\right) - p_i\left(\left(\sum_j p_j y_j^r\right)^2 + \left(\sum_j p_j y_j^i\right)^2\right)\right] = 0 \qquad (3)$$

and

$$\sum_{i=1}^{N} \frac{\partial p_i}{\partial \phi}\left[\left(\sum_j p_j^2\right)\left(y_i^r \sum_j p_j y_j^r + y_i^i \sum_j p_j y_j^i\right) - p_i\left(\left(\sum_j p_j y_j^r\right)^2 + \left(\sum_j p_j y_j^i\right)^2\right)\right] = 0 \qquad (4)$$

The solution to these equations depends on the number of receiver elements, N, their point-spread functions, p, and the signal-to-noise ratio. In general, it will be necessary to solve these equations numerically. However, for high signal-to-noise ratio, it is possible to obtain analytic expressions for the rms tracking errors in the θ and ϕ directions. Firstly, we give a definition of signal-to-noise ratio for an array.

3 SIGNAL-TO-NOISE RATIO DEFINITION

It is not immediately obvious what the definition of signal-to-noise ratio should be for an array of receivers. For a given scene, the signal power, S, could be taken as

$$S = \sum_{i=1}^{N} |\langle y_i \rangle|^2$$

where $\underline{Y}$ is the image vector, and the noise power, N, as

$$N = \sum_{i=1}^{N} \langle |y_i|^2 \rangle$$

with $\underline{Y}$ measured when there are no targets present in the scene.

The difficulty with the above definitions arises when comparison of results relating to different array sizes is made on the basis of equal signal-to-noise ratio since both definitions are themselves functions of array size.

It is proposed, therefore, that comparisons be made between arrays of different size using a given signal-to-noise which depends on the scene and the point-spread functions of the elements only. For a single target in the scene, this is defined as the maximum value of signal-to-noise ratio on a single element as the target is moved across all points in the scene. This definition enables sub-arrays of the total array to be processed without having to redefine the signal-to-noise ratio each time.

4 ANALYTIC SOLUTIONS

Suppose that the position of the single source is at (θ_o,ϕ_o) and the image is corrupted by noise, $\underline{n}$, so that

$$\underline{Y} = \underline{I}_o + \underline{n} \quad , \tag{5}$$

where $\underline{I}_o$ is the noiseless image given by

$$I_{oi} = p_i(\theta_o, \phi_o) \tag{6}$$

and $\underline{n}$ is the noise vector added to the image satisfying

$$\langle |n_i^i|^2 \rangle = \langle |n_i^r|^2 \rangle = \sigma^2/2 \tag{7}$$

For a point-spread function having its maximum at (0,0) the signal-to-noise ratio is

$$p^2(0,0)/\sigma^2$$

For $\sigma^2/p^2\ (0,0) \ll 1$, we look for solutions of (3) and (4) for (θ,ϕ) close to (θ_o,ϕ_o). Expanding $p_i(\theta,\phi)$ in powers of $\varepsilon_\theta = (\theta-\theta_o)$, $\varepsilon_\phi = (\phi-\phi_o)$ using Taylor's theorem gives

$$p_i(\theta,\phi) = p_i(\theta_o,\phi_o) + \varepsilon_\theta \left.\frac{\partial p_i}{\partial \theta}\right|_{\theta_o,\phi_o} + \varepsilon_\phi \left.\frac{\partial p_i}{\partial \phi}\right|_{\theta_o,\phi_o} + \frac{1}{2!}\left(\varepsilon_\theta^2 \left.\frac{\partial^2 p_i}{\partial \theta^2}\right|_{\theta_o,\phi_o} + 2\varepsilon_\theta\varepsilon_\phi \frac{\partial^2 p_i}{\partial\theta\partial\phi} + \varepsilon_\phi^2 \frac{\partial^2 p_i}{\partial \phi^2}\right) + \ldots \quad (8)$$

Using equations (5), (6) and (8) and substituting into equations (3) and (4) gives a pair of simultaneous equations for ε_θ and ε_ϕ

$$\begin{aligned} a_1\varepsilon_\theta + b_1\varepsilon_\phi + c_1 &= 0 \\ a_2\varepsilon_\theta + b_2\varepsilon_\phi + c_2 &= 0 \end{aligned} \quad (9)$$

where

$$a_1 = \sum_i \left.\frac{\partial p_i}{\partial\theta}\right|_{\theta_o,\phi_o} \left\{ p_i(\theta_o,\phi_o) \sum_j p_j^2(\theta_o,\phi_o) \sum_j p_j(\theta_o,\phi_o) \left.\frac{\partial p_j}{\partial\theta}\right|_{\theta_o,\phi_o} - \left.\frac{\partial p_i}{\partial\theta}\right|_{\theta_o,\phi_o} \left(\sum_j p_j^2(\theta_o,\phi_o)\right)^2 \right\}$$

$$b_1 = \sum_i \left.\frac{\partial p_i}{\partial\theta}\right|_{\theta_o,\phi_o} \left\{ p_i(\theta_o,\phi_o) \sum_j p_j^2(\theta_o,\phi_o) \sum_j p_j(\theta_o,\phi_o) \left.\frac{\partial p_j}{\partial\phi}\right|_{\theta_o,\phi_o} - \left.\frac{\partial p_i}{\partial\phi}\right|_{\theta_o,\phi_o} \left(\sum_j p_j^2(\theta_o,\phi_o)\right)^2 \right\}$$

and

$$\langle c_1^2 \rangle = \frac{\sigma^2}{2}\left\{ \left(\sum_j p_j^2(\theta_o,\phi_o)\right)^4 \sum_j \left.\frac{\partial p_j}{\partial\theta}\right|_{\theta_o,\phi_o}^2 - \left(\sum_j p_j^2(\theta_o,\phi_o)\right)^3 \left(\sum_j p_j(\theta_o,\phi_o) \left.\frac{\partial p_j}{\partial\theta}\right|_{\theta_o,\phi_o}\right)^2 \right\}$$

Similarly for a_2, b_2 and $\langle c_2^2 \rangle$.

Solving for ε_θ and ε_ϕ ($a_1b_2 - a_2b_1 \neq 0$) gives:

$$\langle \varepsilon_\theta^2 \rangle = \frac{\sigma^2}{2} \frac{\{f_\phi^2 - Bh_{\phi\phi}\}}{B(h_{\theta\phi}^2 - h_{\theta\theta}h_{\phi\phi}) + f_\phi^2 h_{\theta\theta} - 2f_\phi f_\theta h_{\theta\phi} + f_\theta^2 h_{\phi\phi}} \tag{10}$$

$$\langle \varepsilon_\phi^2 \rangle = \frac{\sigma^2}{2} \frac{\{f_\theta^2 - Bh_{\theta\theta}\}}{B(h_{\theta\phi}^2 - h_{\theta\theta}h_{\phi\phi}) + f_\theta^2 h_{\phi\phi} - 2f_\phi f_\theta h_{\theta\phi} + f_\phi^2 h_{\theta\theta}} \tag{11}$$

with $\langle \varepsilon_r^2 \rangle$, defined as $\langle \varepsilon_\theta^2 \rangle + \langle \varepsilon_\phi^2 \rangle$, given by

$$\langle \varepsilon_r^2 \rangle = \frac{\sigma^2}{2} \frac{(f_\theta^2 + f_\phi^2 - B(h_{\theta\theta} + h_{\phi\phi}))}{B(h_{\theta\phi}^2 - h_{\theta\theta}h_{\phi\phi}) + f_\theta^2 h_{\phi\phi} - 2f_\phi f_\theta h_{\theta\phi} + f_\phi^2 h_{\theta\theta}} \tag{12}$$

where

$$B = \sum_j p_j^2(\theta_o,\phi_o), \quad f_\theta = \sum_j p_j(\theta_o,\phi_o) \left.\frac{\partial p_j}{\partial \theta}\right|_{\theta_o,\phi_o},$$

$$f_\phi = \sum_j p_j(\theta_o,\phi_o) \left.\frac{\partial p_j}{\partial \phi}\right|_{\theta_o,\phi_o}, \tag{13}$$

$$h_{\theta\theta} = \sum_j \left.\frac{\partial p_j}{\partial \theta}\right|^2_{\theta_o,\phi_o}, \quad h_{\phi\phi} = \sum_j \left.\frac{\partial p_j}{\partial \phi}\right|^2_{\theta_o,\phi_o}, \quad h_{\theta\phi} = \sum_j \left.\frac{\partial p_j}{\partial \theta}\right|_{\theta_o,\phi_o} \left.\frac{\partial p_j}{\partial \phi}\right|_{\theta_o,\phi_o}$$

The expressions for the rms errors given here are valid for any array configuration and any element point-spread function in the limit of large signal-to-noise ratio. For an array with elements symmetrically placed in the θ and ϕ directions about the origin and each element with a symmetrical point-spread function, equations (10) and (11) simplify considerably for a target on boresight to give

$$\langle \varepsilon_\theta^2 \rangle = \frac{\sigma^2/2}{\sum_j \left(\left.\frac{\partial p_j}{\partial \theta}\right|_{o,o}\right)^2}$$

$$\langle \varepsilon_\phi^2 \rangle = \frac{\sigma^2/2}{\sum_j \left(\left.\frac{\partial p_j}{\partial \phi}\right|_{o,o}\right)^2} \tag{15}$$

which shows the dependence of the tracking errors on the gradients of the point-spread functions at the origin. In section 6 we shall evaluate these expressions for particular array configurations but first we give a short description of a numerical routine to find targets in a scene which is used together with the analytic results in this report to illustrate some array properties.

5 NUMERICAL SIMULATION

A numerical algorithm has been written which takes a complex image vector and searches the scene for point sources. The solution for the amplitudes, positions and phases of the sources is the one which minimises the error between the image and the image of the solution (equation (1)). This is obtained by using a nonlinear least squares algorithm (the Levenberg-Marquardt method) with a starting value provided by first performing a coarse search in position for the sources. In order to obtain the rms error in position for a single target, repeated solutions are made using a different noisy image each time. The noise is generated by using a pseudo-random number generator to produce a Gaussian distribution and hence a noise vector which is added to the image without noise after each solution. The rms error is estimated on the basis of 500 solutions.

6 EXAMPLES

a. Linear Array

Consider an array of $(2\ell+1)$ elements positioned at $\theta = 0, \pm\pi, \ldots, \pm\ell\pi$, each with point-spread function

$$p_i(\theta) = \frac{\sin(i\pi-\theta)}{i\pi-\theta} \tag{16}$$

so that the elements are at the Nyquist separation (Figure 1). For a linear array, the mean square error in position for high signal-to-noise ratio is given by

$$\langle\varepsilon_\theta^2\rangle = \frac{\sigma^2/2}{\left|\sum_j\left(\frac{\partial p_j}{\partial\theta}\Big|_{\theta_o}\right)^2 - \sum\left(p_j(\theta_o)\frac{\partial p_j}{\partial\theta}\Big|_{\theta_o}\right)^2 \Big/ \sum p_j^2(\theta_o)\right|} \tag{17}$$

which may be evaluated for a target at the array centre, using (16) to give

$$\langle\varepsilon_\theta^2\rangle = \sigma^2 \Big/ 4\sum_{i=1}^{\ell}\frac{1}{i^2\pi^2} \tag{18}$$

Thus, the rms error is inversely proportional to the square root of the signal-to-noise ratio (defined, according to section 3, as $p^2(0)/\sigma^2 = \sigma^{-2}$) and <u>decreases</u> as the number of elements <u>increases</u>.

The variation of rms error in position with target position can be determined by evaluating (17). Figures 2a-c plot $\sqrt{(\langle\varepsilon_\theta^2\rangle/\sigma^2)}$ as a function of target position for 3, 5 and 7 element arrays. Only the region $\theta > 0$ is plotted as the function is symmetrical about the array centre. The positions of the elements are at $0, \pm\pi, \ldots, \pm\ell\pi$. The figures show that the error is approximately constant while the target is within the bounds of the array but increases sharply outside the array.

The dotted lines in Figures 2a-c illustrate the situation where the two elements nearest to the position of the target are used to estimate target position, rather than all the elements. There is a degradation in tracking accuracy, particularly at the points where the target position moves from one pair of points to another, though this is not very significant. In practice, in the presence of noise, it may not be known which are the two array elements nearest to the target position, particularly when the target is near a boundary of the region. Therefore, it may be expected that the error is worse than that shown. For a seven element array (Figure 2c), the ratio of the rms error at the origin using pairs of elements to that using all the elements is 1.65. Thus, tracking using pairs of elements could require up to an additional 4.35 dB of signal-to-noise ratio to give equal performance to that of the whole array.

(NB. The expression given by equation (17) is valid provided $\sigma^2/\Sigma\ p_j^2(\theta_o) \ll 1$. However, this approximation breaks down at points outside the array where $\Sigma\ p_j^2(\theta_o) = 0$, ie at multiples of π for the sin(x)/x point-spread function used here.)

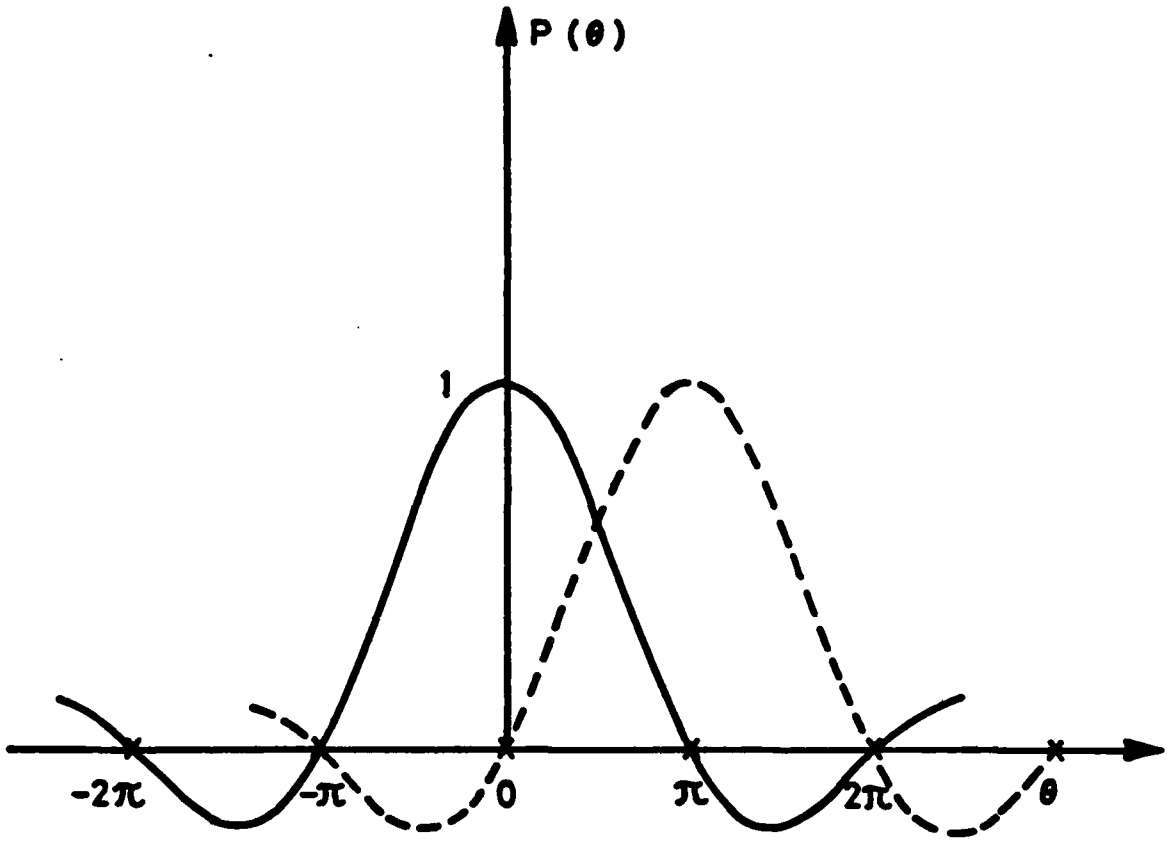

FIG.1 POINT-SPREAD FUNCTIONS AND SPACING OF ELEMENTS OF A LINEAR ARRAY OF RECEIVERS

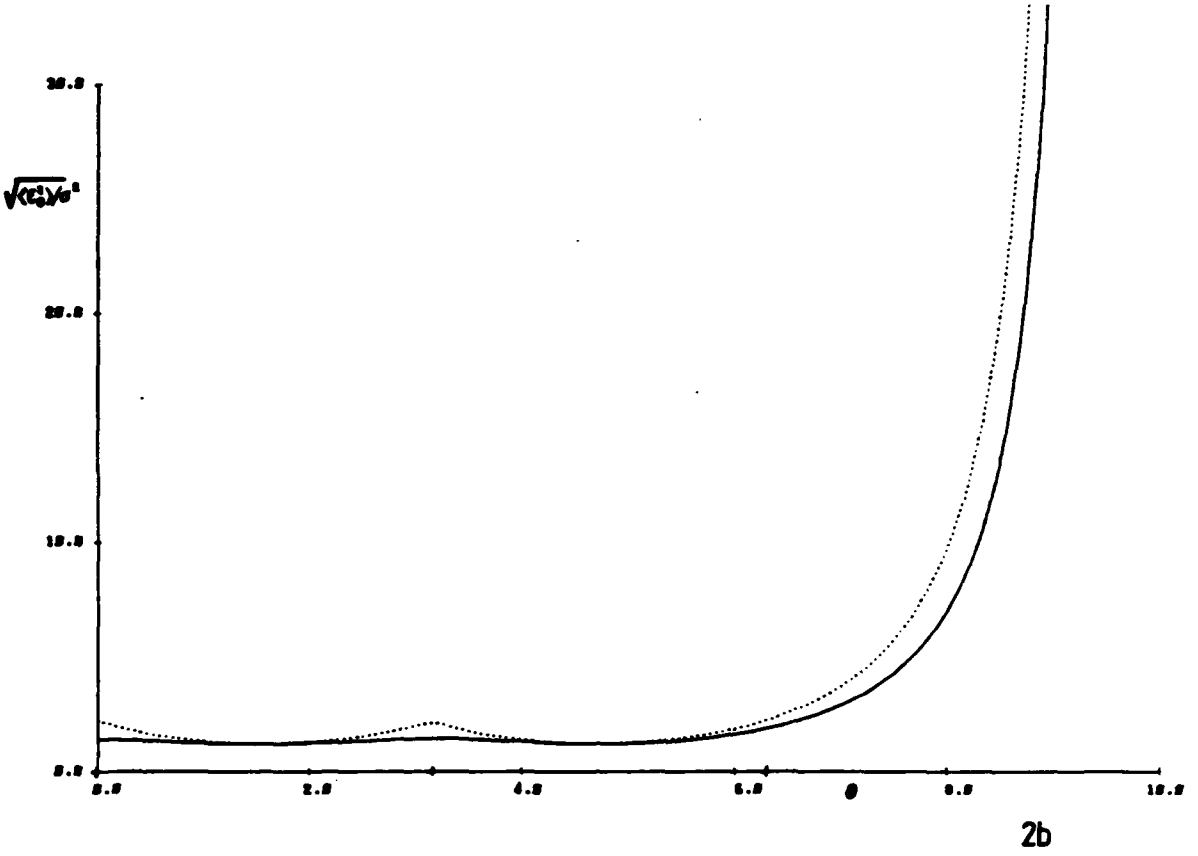

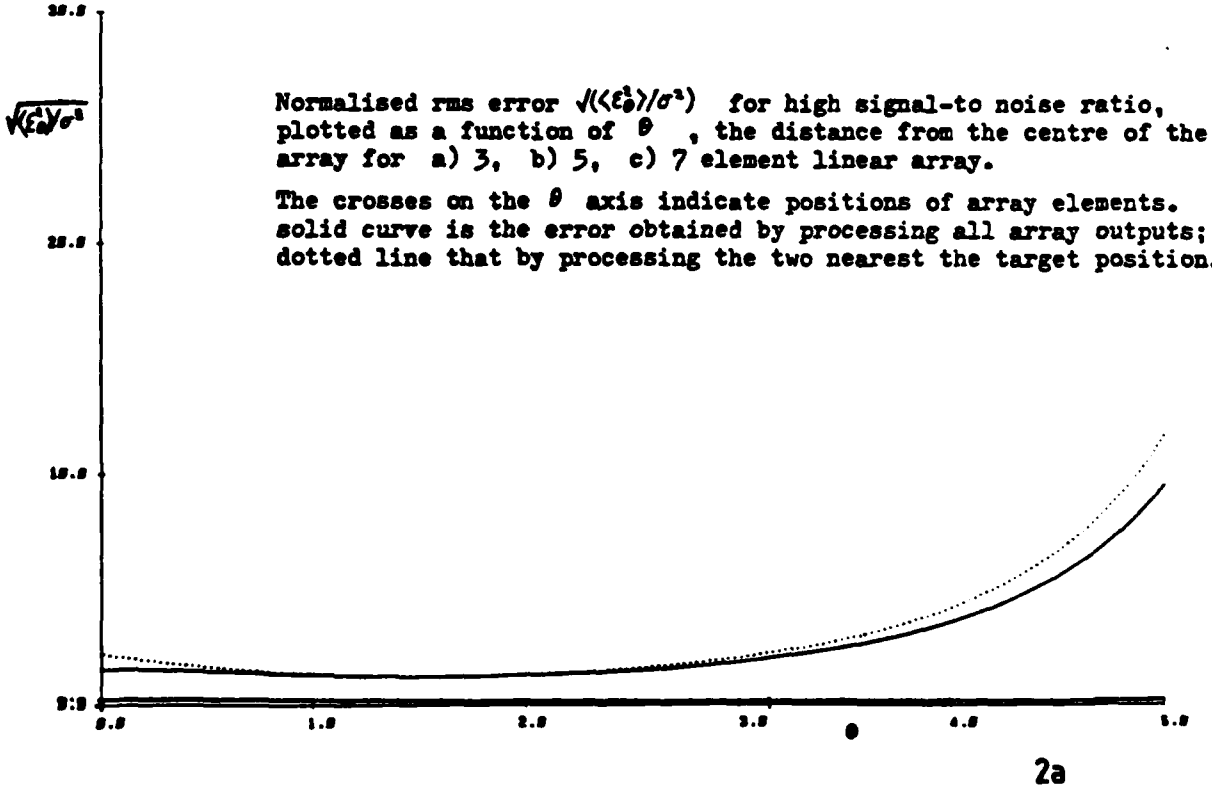

Normalised rms error $\sqrt{(\langle \varepsilon_\theta^2 \rangle / \sigma^2)}$ for high signal-to noise ratio, plotted as a function of θ, the distance from the centre of the array for a) 3, b) 5, c) 7 element linear array.

The crosses on the θ axis indicate positions of array elements. The solid curve is the error obtained by processing all array outputs; the dotted line that by processing the two nearest the target position.

FIGURE 2

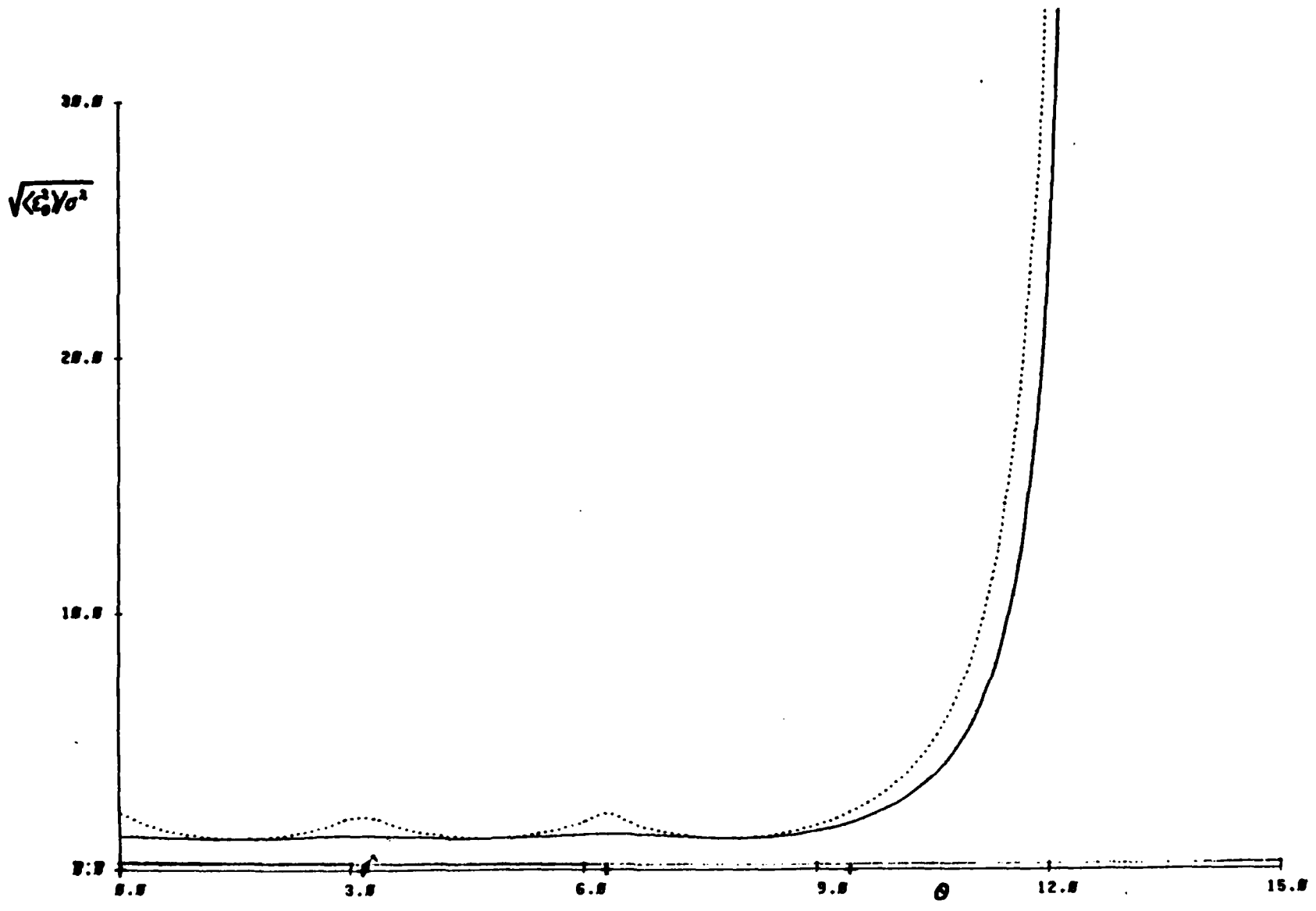
30.0
$\sqrt{\langle \xi_0^2 \rangle \sigma^2}$
20.0
10.0
0.0
0.0
3.0
6.0
9.0
θ
12.0
15.0

10

2c

b. Square Lattice

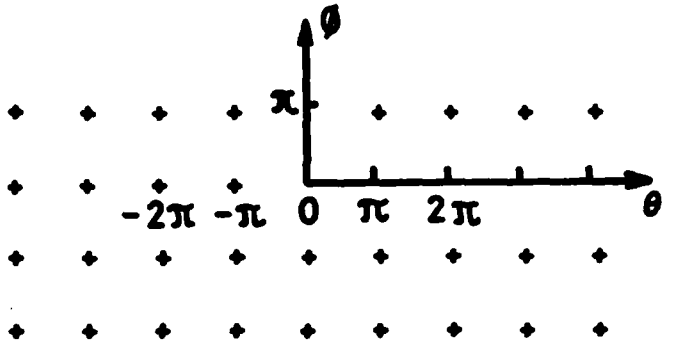

FIG. 3

For an array of receivers with circularly symmetric point-spread functions given by

$$p_i(\theta,\phi) = J_1(r)/r$$

where $r^2 = \theta^2 + \phi^2$, positioned on a square lattice at points $(\theta,\phi) = (m\pi,n\pi)$, $-\ell < m,n < \ell$, (see Figure 4) the rms error in position has been evaluated as a function of array size and target position. This is shown in Figures 4a-c where $\sqrt{(<\varepsilon_r^2>/\sigma^2)}$ is plotted as a function of θ for various value of ϕ for 3 x 3, 5 x 5 and 7 x 7 arrays centred on the origin. For a source which lies within the boundaries of the array the error varies little across the array but increases outside. Figure 5 plots the error as a function of signal-to-noise ratio for a 7 x 7 and 3 x 3 array for a target at the origin and compares it with the error produced by using the four nearest elements (taken to be at (0,0), (0,π), (π,0) and (π,π)) to estimate position. Figures 4 and 5 show that for a 2 x 2 sub-array to maintain a constant tracking error over the array equivalent to the larger 7 x 7 array, then up to 4.5 dB extra signal-to-noise ratio is required. For low signal-to-noise ratios, it is expected that the differences in performance between the arrays would be small.

c. Hexagons

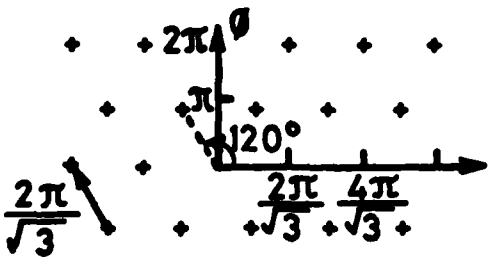

FIG. 6a

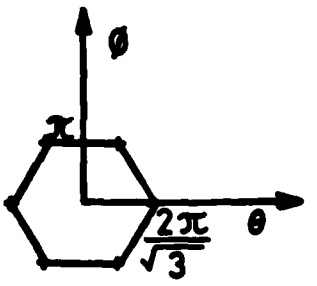

FIG. 6b

It has been shown elsewhere (Webb and Hearn, 1984; Petersen and Middleton, 1962) that the optimum sampling lattice for a two dimensional isotropic function, such as $J_1(r)/r$, is based on a lattice of equilateral triangles (Figure 6a). This allows the image plane to be sampled with a lower density of elements. Results are presented here for an hexagonal array of seven elements (Figure 6b). The variation of the rms errors with target position are plotted in Figures 7a-c as a function of θ for various values of ϕ. As might be expected, there are differences between the figures for $\langle \varepsilon_\theta^2 \rangle$ and $\langle \varepsilon_\phi^2 \rangle$ due to asymmetry. Also in Figure 7 are plotted results of the numerical simulation evaluated for a signal-to-noise ratio of 2.5×10^5. Again there is very good agreement between the simulation and the theory for high signal-to-noise ratio.

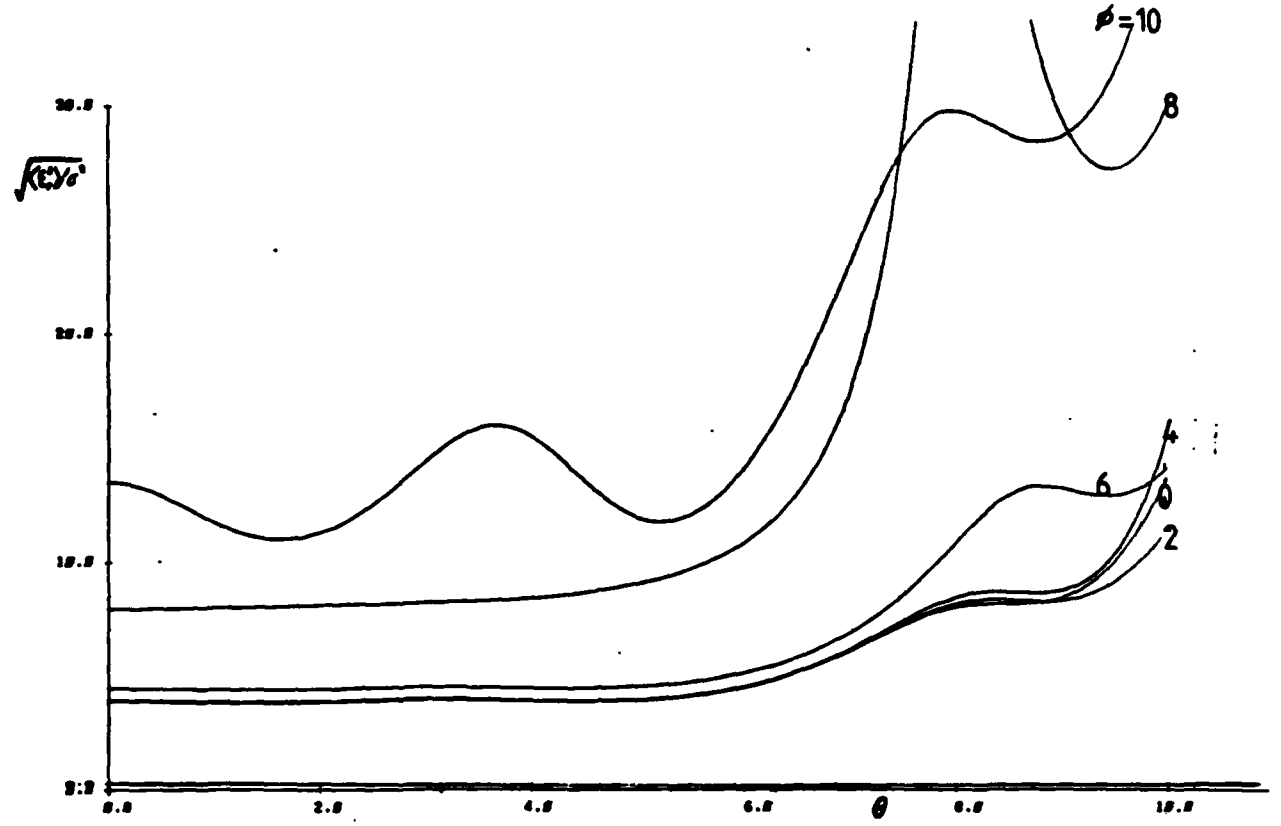

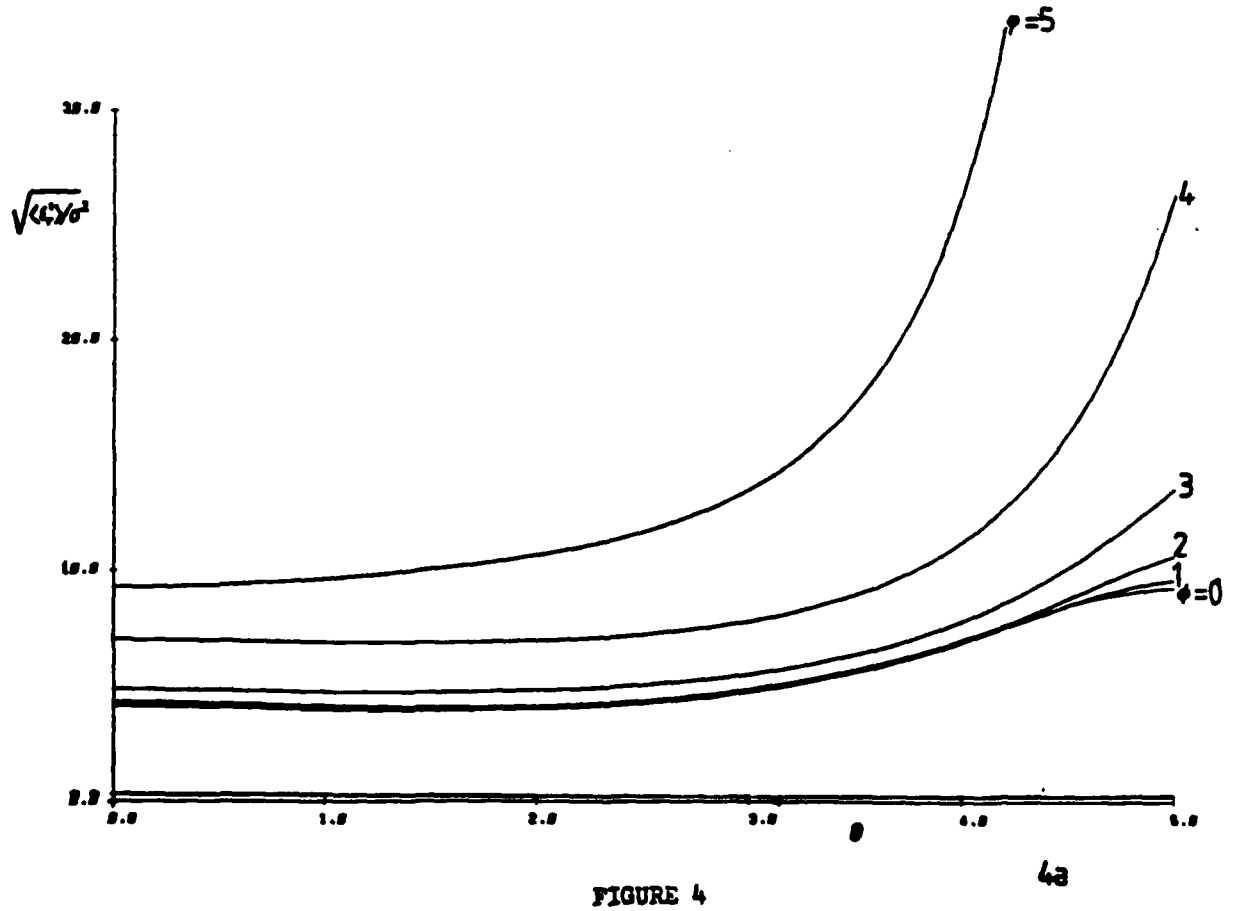

FIGURE 4

Normalised error $\sqrt{\langle \epsilon_\phi^2 \rangle}/\sigma^2$ plotted as a function of θ for various ϕ for a) 3 x 3, b) 5 x 5 and c) 7 x 7 square array.

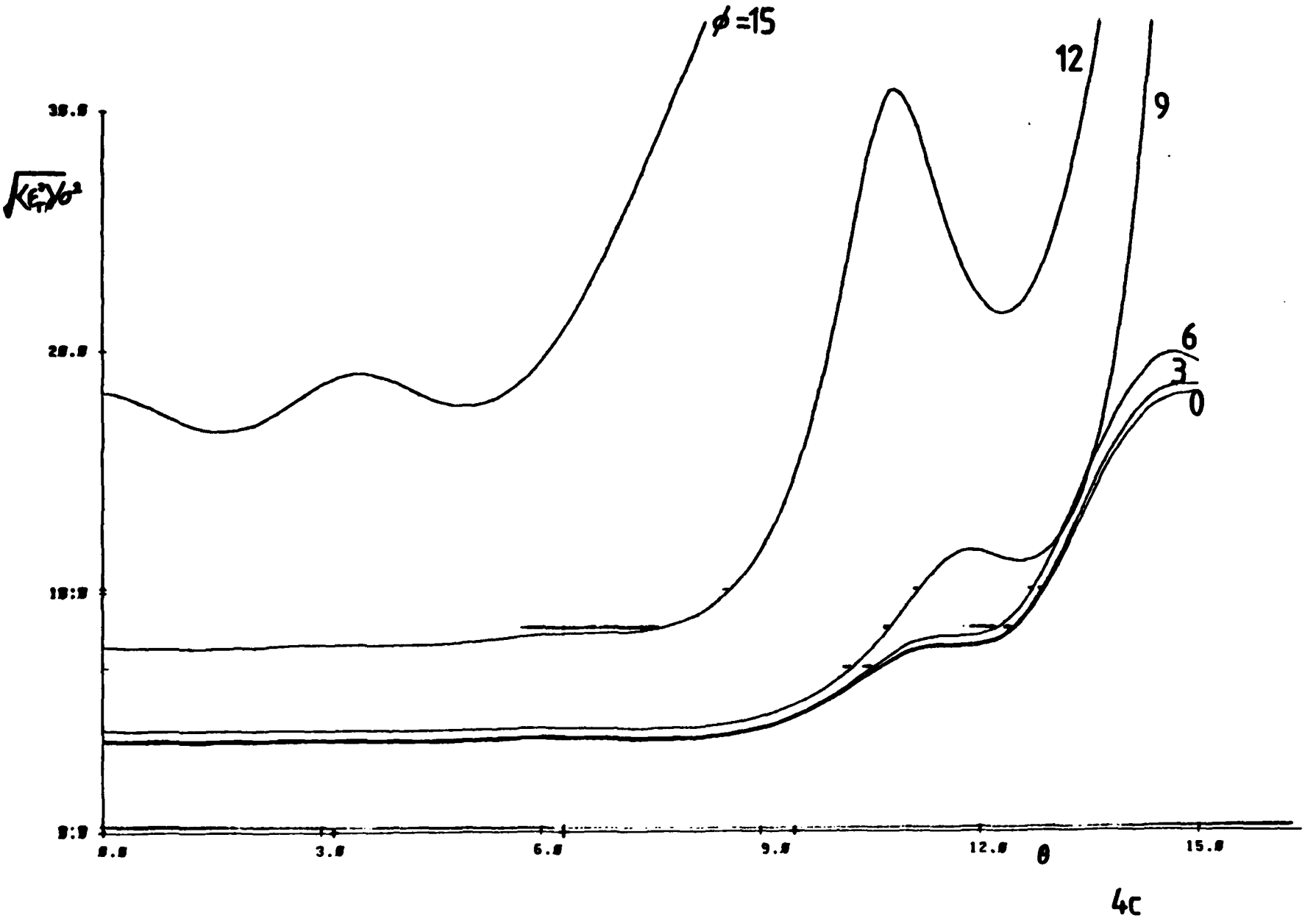

4c

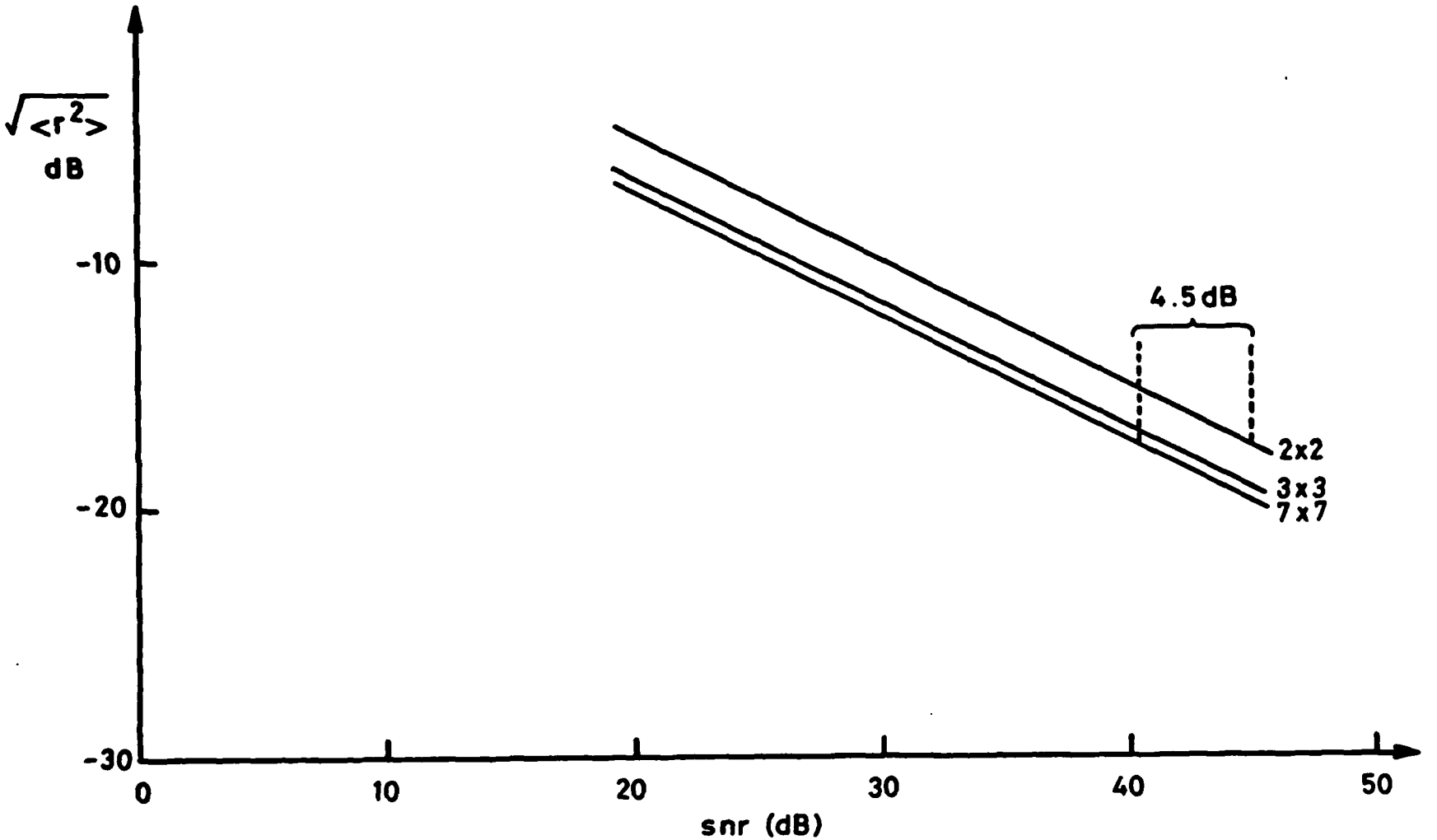

FIG.5 RMS ERROR IN POSITION AS A FUNCTION OF SIGNAL-TO-NOISE RATIO FOR THE TARGET ON THE ORIGIN OF A 7x7 ARRAY. FOR COMPARISION, THE ERROR OBTAINED USING A 3x3 AND A 2x2 SUB-ARRAY IS ALSO SHOWN.

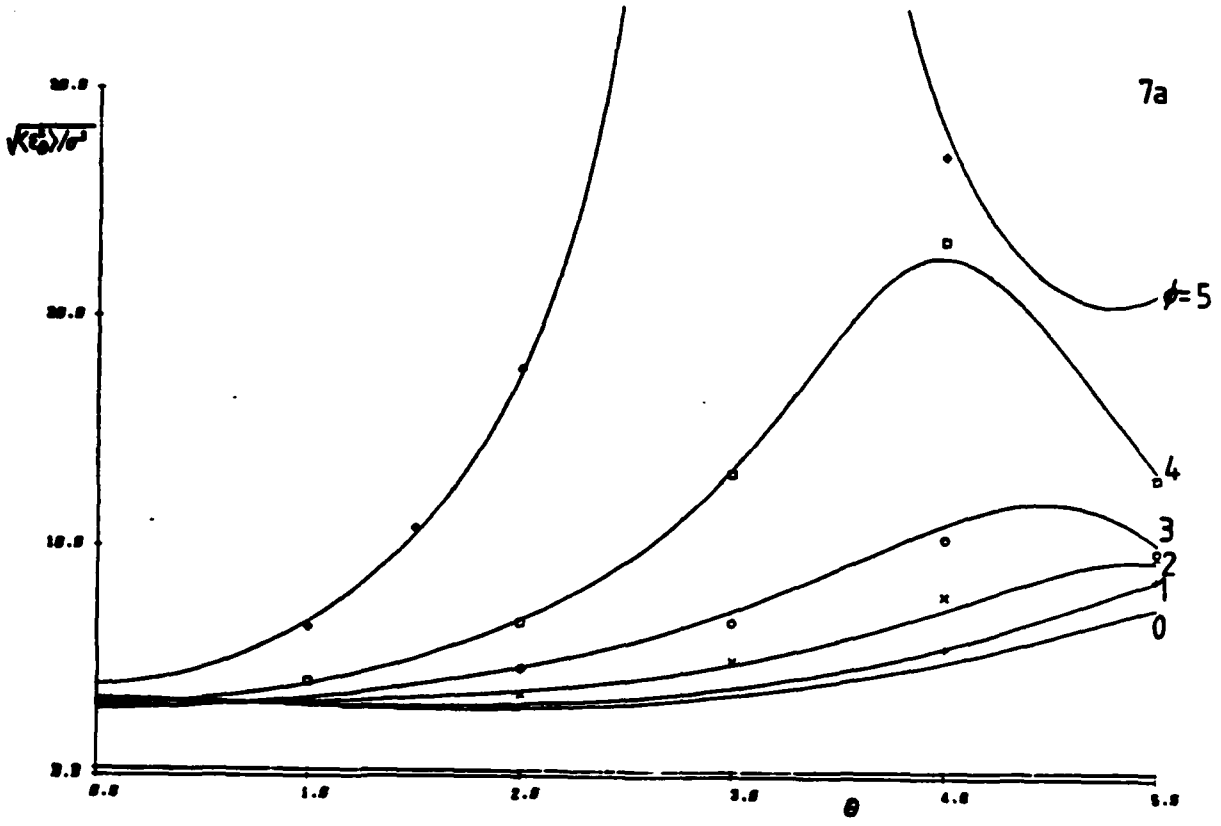

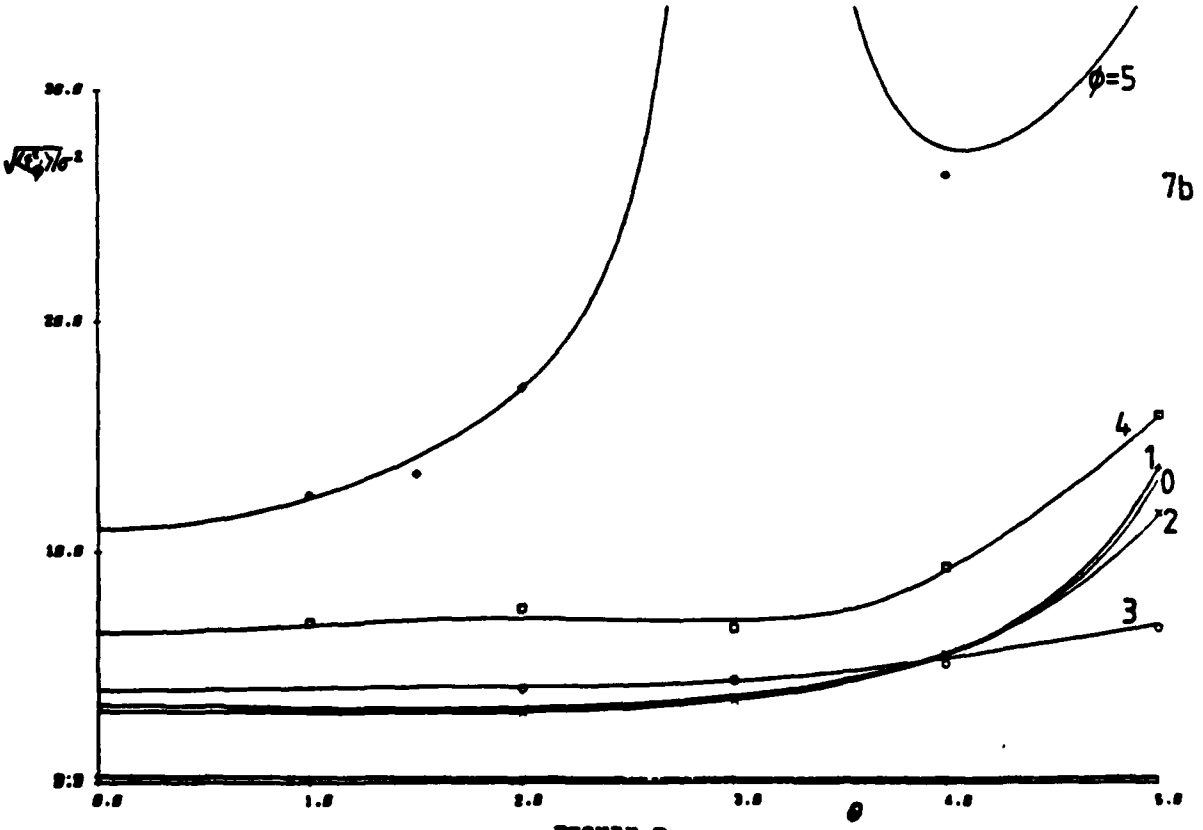

FIGURE 7

Normalised errors: a) $\sqrt{\langle \xi_\theta^2 \rangle/\sigma^2}$ b) $\sqrt{\langle \xi_\phi^2 \rangle/\sigma^2}$ and c) $\sqrt{\langle \xi_r^2 \rangle/\sigma^2}$
for a seven element hexagonal array as a function of θ for various values of ϕ .

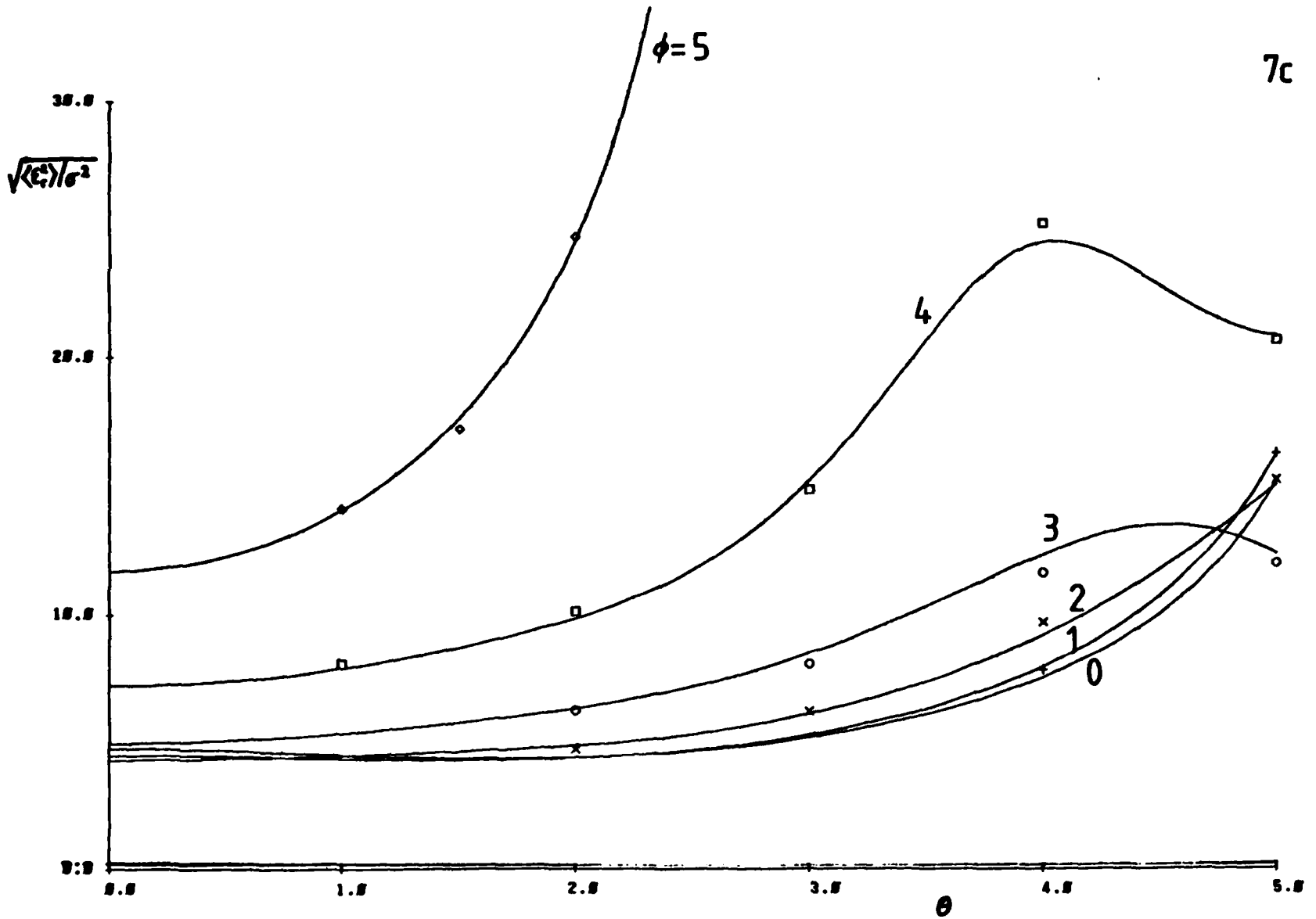
7c
ϕ=5
4
3
2
1
0
$\sqrt{\langle E_T^2 \rangle / \sigma^2}$
30.0
20.0
10.0
0.0
0.0
1.0
2.0
3.0
4.0
5.0
θ

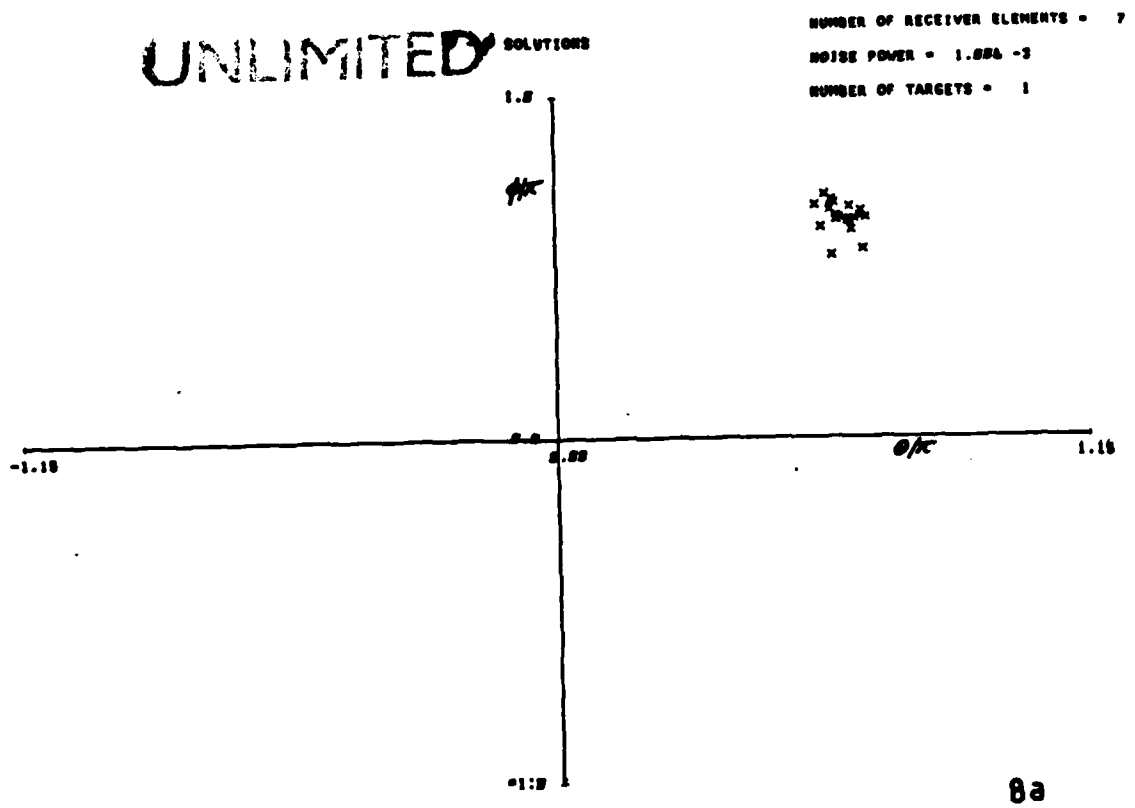

8a

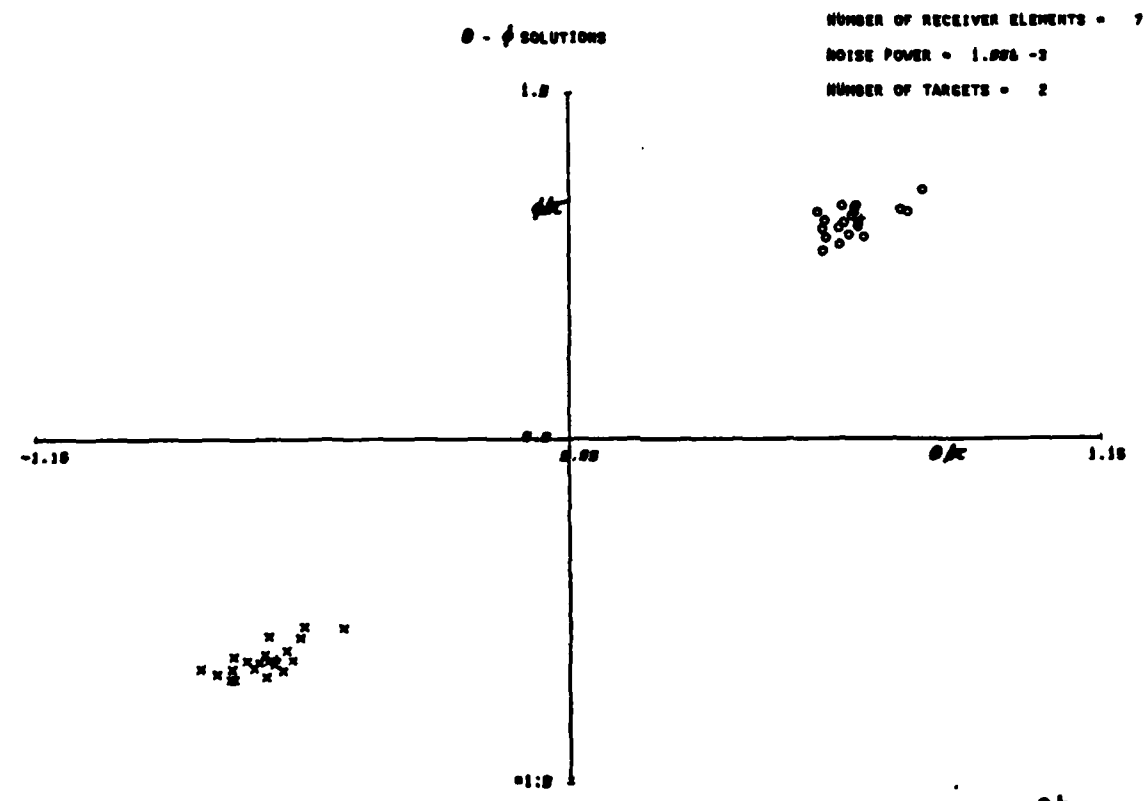

8b

FIGURE 8

Solutions of the numerical algorithm plotted in the θ-ϕ plane for a seven element hexagonal array for: a) a single source at (2,2)
b) two sources at (2,2) and (-2,-2)
The signal-to-noise ratio is 2.5×10^2.

7 DISCUSSION

The tracking error for a single target as viewed by an array of receivers has been determined analytically as a function of position for high signal-to-noise ratios. These results have been supplemented by a Monte-Carlo simulation which uses a numerical algorithm (Levenberg-Marquardt method) to solve repeatedly the set of nonlinear simultaneous equations and estimate the rms error in position. The results show that using more than the two receiver outputs allowed by monopulse then the tracking error may be maintained at an approximately constant level across the plane of the array, but the error does not reduce significantly as more elements are processed. The increase in error due to processing two elements only corresponds to, at most, a 4.5 dB reduction in signal-to-noise ratio.

The numerical method has been developed to search a scene for many targets and Figures 8a, b show 20 separate solutions for a single target and two-target scenes for a seven element hexagonal array (see section 5c). The signal-to-noise ratio is $p^2(0,0)/\sigma^2$, which is $1/4\sigma^2$ for the spherically symmetric beam-shape $J_1(r)/r$ (2.5×10^2 for a noise power of 10^{-3}).

Further work in this area will concentrate on analysing the outputs produced by more complex scenes and the ability of arrays to resolve unwanted sources. In addition, optimising the point-spread function and element spacing for single target tracking will be considered.

8 CONCLUSIONS

Processing the outputs from an array of receivers does have definite advantages over processing pairs of elements only. It allows a target to be tracked smoothly across the plane of the array, reducing the error in the neighbourhood of elements. An array based on a structure of equilateral triangles gives similar results to one based on a square lattice but covers a wider field of view for a given number of receiver elements.

ACKNOWLEDGEMENTS

Acknowledgement is made to M Stephens of Plessey, Roke Manor, for helpful comments and suggestions.

REFERENCES

1 Webb A R, Hearn D B and Sleigh A C, Resolution of Point Sources Using Linear Arrays, RSRE Memo 3587, 1984.

2 Webb A R, and Hearn D B, Sampling Images in Two Dimensions, SP4 Division Research Note, February 1984.

3 Petersen D P and Middleton D, Sampling and Reconstruction of Wave-number-limited Functions in N-Dimensional Euclidean Spaces, Information and Control 5, 279-323, 1962.

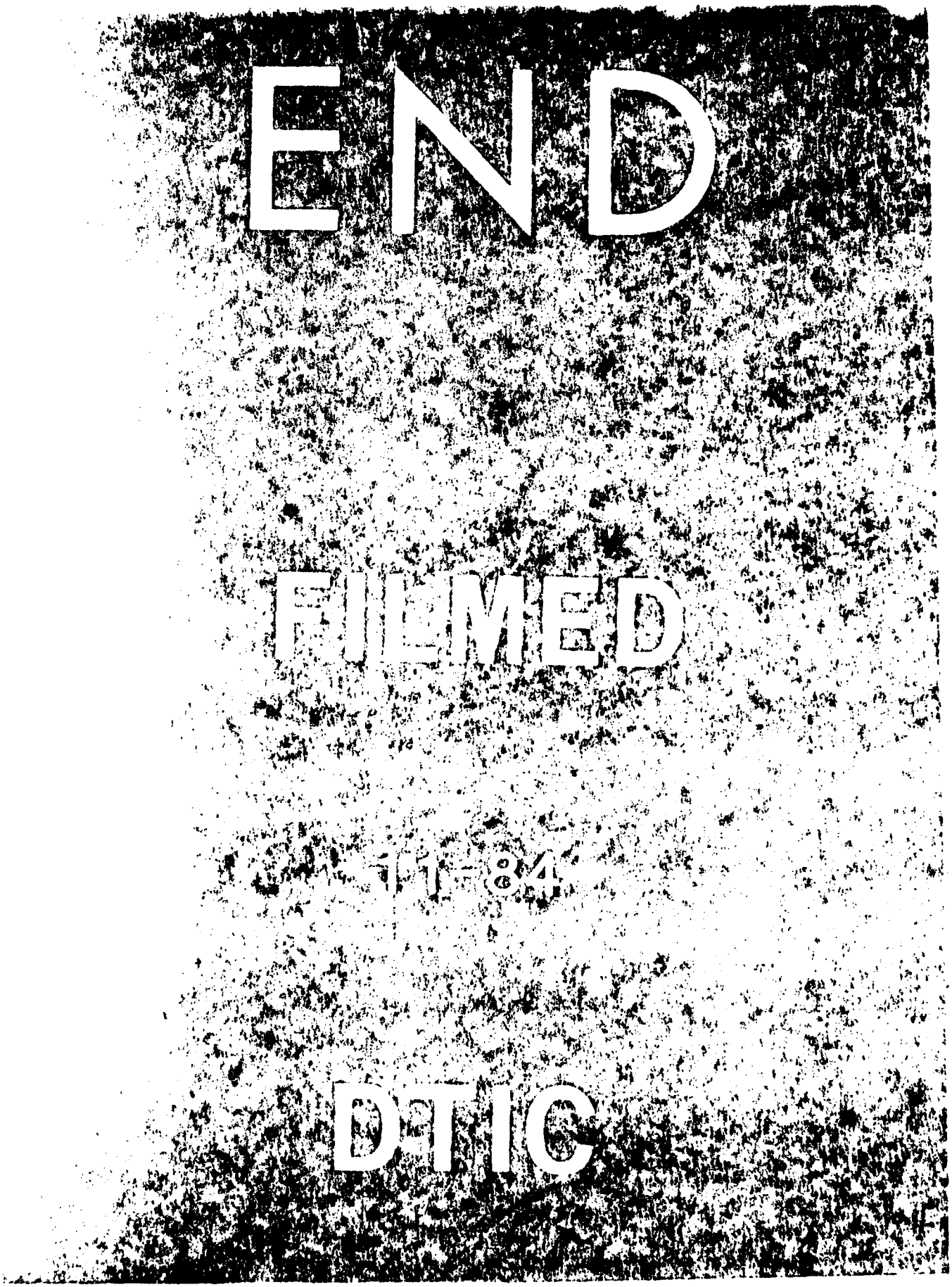
END
FILMED
6-84
DTIC